A SPECIALIZED MULTIPARTICLE SPECTROMETER

B. Gittelman†
Stanford Linear Accelerator Center

ABSTRACT

A detection system is described for measuring cross sections for peripheral processes in which the high-momentum forward particle is hadronically stable.

I. INTRODUCTION

High-energy reactions are characterized theoretically as proceeding through the exchange of particle systems or field quanta. Consider the two-body reaction

$$A + B \rightarrow C + D, \tag{1}$$

where A is the incident projectile, B the stationary target, and C, D are stable or unstable final particles. Current theoretical attempts to understand the systematics of these reactions begin with the schematic conceptualization shown in the diagram.

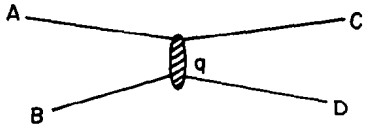

The transformation of A into C takes place with the emission or absorption of the particle system of 4-momentum q. Considerations of the properties of propagators guarantee that the differential cross section will peak at small values of q^2. From this we know that C will preferentially be emitted into the laboratory at a small angle with respect to the incident beam and with a momentum which is comparable to that of the incident beam.

Factorization is the statement that the amplitude for the process can be written as a product of terms, one having to do with the dynamics of the A-C vertex and another the B-D vertex. If factorization holds, one can expect to relate the different

processes which proceed through the exchange of the same system. Much work has been done on this during the past half dozen years, with some partial success. The exhortations of phenomenologists working in this field are:

1. It is important to obtain accurate data on many reactions.

2. The theorists need both the energy and angular dependence of the cross sections.

3. The energy dependence should be measured over the widest range possible. They hope the number of systems that can be exchanged is reduced to unity at the highest energy.

Since most of the cross section is concentrated near the region of minimum momentum transfer, it seems obvious to measure in this region. It is possible to build a multiparticle spectrometer detector system (abbreviated MSDS) to simultaneously measure a large class of two-body reactions in the high-energy, low-momentum-transfer kinematic region. There is a natural design choice which can be made depending on the properties of particle C:

1. Charged and Stable
2. Neutral and Stable
3. Charged and Unstable
4. Neutral and Unstable.

All four cases contain many interesting and important reactions to study. However, in this note we will limit the discussion to case 1 in which case particle C is a $\pi^{\pm}$, $K^{\pm}$, p, or $\bar{p}$.

The general idea is to pass a charged particle beam of well-defined momentum through a hydrogen target. The particles in the beam will be identified upstream of the target by a set of differential Cerenkov counters. A high-momentum, small solid-angle magnetic spectrometer would be set up downstream of the target to measure the momentum and angle of particle C. Particle C will be identified by the use of a series of threshold Cerenkov counters behind the magnetic spectrometer. A second magnetic spectrometer will surround the hydrogen target to measure the momentum and angle of particle D or its charged decay products. This latter spectrometer will intercept almost 4π steradians and handle momenta up to 1.5 to 2 GeV/c. (This type of device has been referred to in the Summer Study as a vertex detector.)

Before going into some of the details of an MSDS design, it is a good idea to have fixed a list of possible reactions which would be studied. Toward this end, we have drawn up such a list. Remembering that we write the reaction A + B → C + D where C has high laboratory momentum, we can separate the reactions into those involving meson exchange (small t) and those involving baryon exchange (small u).

Table I. Reactions to Study.

	Meson Exchange		Baryon Exchange
1.	$\pi^{\pm} + p \rightarrow \pi^{\pm} + p$	15.	$\pi^{\pm} + p \rightarrow p + \pi^{\pm}$
2.	$K^{\pm} + p \rightarrow K^{\pm} + p$	16.	$K^{+} + p \rightarrow p + K^{+}$
3.	$\bar{p} + p \rightarrow \bar{p} + p$	17.	$\bar{p} + p \rightarrow p + \bar{p}$
4.	$p + p \rightarrow p + p$	18.	$\pi^{\pm} + p \rightarrow p + \rho^{\pm}$
5.	$\pi^{\pm} + p \rightarrow \pi^{\pm} + N^{*+}$	19.	$\pi^{\pm} + p \rightarrow p + A_1^{\pm}$
6.	$\pi^{\pm} + p \rightarrow K^{+} + \Sigma^{\pm}$	20.	$\pi^{\pm} + p \rightarrow p + B^{\pm}$
7.	$\pi^{\pm} + p \rightarrow K^{+} + Y^{*\pm}$	21.	$\pi^{\pm} + p \rightarrow p + A_2^{\pm}$
8.	$K^{\pm} + p \rightarrow K^{\pm} + N^{*+}$	22.	$K^{+} + p \rightarrow p + (K^{*})^{+}$
9.	$K^{-} + p \rightarrow \pi^{-} + \Sigma^{+}$	23.	$\bar{p} + p \rightarrow \pi^{\pm} + \pi^{\mp}$
10.	$K^{-} + p \rightarrow K^{+} + \Xi^{-}$	24.	$\bar{p} + p \rightarrow K^{-} + K^{+}$
11.	$K^{-} + p \rightarrow \pi^{-} + Y^{*+}$	25.	$\bar{p} + p \rightarrow \pi^{\pm} + (\text{Boson})^{\mp}$
12.	$K^{-} + p \rightarrow K^{+} + \Xi^{*-}$	26.	$\bar{p} + p \rightarrow K^{-} + K^{*+}$
13.	$\bar{p} + p \rightarrow \bar{p} + N^{*+}$	27.	$\bar{p} + p \rightarrow p + \overline{N^{*-}}$
14.	$p + p \rightarrow p + N^{*+}$		

The above list consists of only those reactions using proton targets. There is of course a similar list for neutron targets. We should point out that for most of the reactions that have been written down, particle D is unstable. This is the reason for building the "vertex detector." Once we have made the investment in this large solid-angle device, in order to have reaction identification, we obtain an important additional return for free. For those reactions in which the low-momentum recoil (particle D) has spin greater than 1/2, it is important to measure its polarization. A measurement of the angular distribution of its decay modes enables one to make a partial determination of the density matrix of the polarization.

II. AN APPROPRIATE BEAM LINE

D. Reeder has designed a "high-quality unseparated beam" (see SS-41) which appears to be a good start. We will assume that this is the beam that we want to use. For completeness we list the important properties at the hydrogen target. The numbers come from the 2.5-mrad beam taken from 3×10^{12} protons per pulse incident on 4 cm of tungsten.

Table II. Beam Properties at the Target.

Vertical Height	±7 mm
Vertical Divergence	±0.06 mrad
Horizontal Width	±1.5 mm
Horizontal Divergence	±0.1 mrad
$(\Delta p/p)_{min}$ (Note: not clear from text why we cannot get ±0.02%)	±0.05%
$(\Delta p/p)_{max}$	±2%

Typical rate for $\Delta p/p = 0.1\%$ (see Fig. 3 of SS-41 for better numbers)

$\pi^{\pm}$	1.5×10^6/pulse
K^+	5×10^4/pulse
K^-	1.5×10^4/pulse
$\bar{p}$	10^4/pulse
p	Variable depending on whether one tunes for the quasi-elastic peak

Assuming a 1-second spill time, the rates in this beam are sufficiently low to do particle identification using upstream Cerenkov counters. Since the angular divergence in the beam is very small, it does not appear to be unreasonable to expect a factor of 10^3 (possibly 10^4) separation of K's from π's at 100 GeV/c. Two differential Cerenkov counters (triple ring focus) in series will give adequate identification.

The angular divergence of the indicent beam is sufficiently small that we can neglect its contribution to the error in the production angle. At 100 GeV/c it introduces an uncertainty in the momentum transfer of $\simeq 10^{-2}$ GeV/c which is not important for our purposes. The momentum resolution in the beam, as we shall see, is also adequate.

III. FORWARD HIGH-MOMENTUM, SMALL SOLID-ANGLE MAGNETIC SPECTROMETER

We want to be able to use the forward spectrometer to kinematically identify the process. For example, the spectrometer should separate the reactions

$$\pi^- + p \rightarrow p + \pi^-$$
$$\rightarrow p + \rho^-$$
$$\rightarrow p + A_1^-$$
$$\text{etc.}$$

An approximate relation between the change in the proton momentum with the mass of particle D for low momentum transfer is

$$\frac{dp_c}{dM_D^2} \simeq -\frac{1}{2M_B} . \qquad (2)$$

Making up a list for these reactions:

Particle D	Δp_{proton}
π^-	0.01 GeV/c
ρ^-	0.31
A_1^-	0.58
B^-	0.84

We see that a momentum resolution of 0.15 GeV/c (i.e., ±0.075) will separate the different products. Since the incident beam monochromaticity is ≃ 0.1 GeV/c at 100 GeV/c we should design the spectrometer to have similar resolution; thus one design criteria is $\delta p/p = 10^{-3} = \pm 0.5 \times 10^{-3}$. One can make a similar argument for $\delta p/p = 10^{-3}$ using the reaction series

$$\begin{aligned} \pi + p &\rightarrow \pi + p \\ &\rightarrow \pi + (p\pi) \\ &\rightarrow \pi + N^*(1238) \\ &\rightarrow \pi + N^*(1470) \\ &\rightarrow \pi + N^*(1520) \\ &\rightarrow \pi + N^*(1550) \\ &\rightarrow \pi + N^*(1688) \end{aligned}$$

Only the N^* (1520) will crowd the picture.

From the resolution, the maximum useful momentum, and the maximum magnetic field we can choose a spectrometer length. We have already taken p_{max} to be 100 GeV/c. We take B_{max} = 15 kG where we can be confident that saturation effects will not destroy the uniform field optics. To decide on an optimal length, we can consider the spectrometer system as being made up of 3 sections as shown in Fig. 1. Regions 1 and 3 consist of a set of wire-plane spark chambers separated by distances ℓ_1 and ℓ_3. The magnetic field extends over a distance ℓ_2 between regions 1 and 3. We assume the spark chambers have 1 mm wire spacing, so that the root mean square spatial resolution is $\delta y = \pm 0.3$ mm = 0.6 mm. The measured bend angle is given by

$$\Theta = \frac{y_D - y_C}{\ell_3} - \frac{y_B - y_A}{\ell_1} , \tag{3}$$

so that the error in this angle is

$$\delta\Theta = \frac{\sqrt{2}}{\ell_1 \ell_3} \left\{ \ell_1^2 + \ell_3^2 \right\}^{1/2} \delta y . \tag{4}$$

The resolution is related to the measuring error by

$$\frac{\delta p}{p} = \frac{\delta\Theta}{\Theta} = \sqrt{2} \, \frac{\left\{ \ell_1^2 + \ell_3^2 \right\}^{1/2}}{\ell_1 \ell_3} \, \delta y \, \frac{p}{\ell_2 eB} . \tag{5}$$

One can play games with the ratio ℓ_1/ℓ_3 if there are additional conditions to satisfy. In particular, setting $\ell_3 >> \ell_1$ will improve the resolution by a factor of $\sqrt{2}$ or allow a 20% reduction in ℓ_1 and ℓ_2. However, since we are concerned about keeping the overall length small (Cerenkov counters must go behind the last wire plane), we take $\ell_1 = \ell_3$ and get

$$\frac{\delta p}{p} = \frac{2\delta y}{\ell_1 \ell_2} \, \frac{p}{eB} . \tag{6}$$

This is fixed relation between ℓ_1 and ℓ_2 which is required for the resolution:

$$\ell_1 = \frac{2(\delta y)}{\ell_2} \, \frac{p}{eB} \, \frac{1}{(\delta p/p)} \tag{7}$$

$$= \frac{2(0.6 \times 10^{-3})}{\ell_2} \, \frac{100 \times 10^9}{1.5 \times 3 \times 10^8} \, \frac{1}{10^{-3}}$$

$$\ell_1 = \frac{268}{\ell_2} . \tag{8}$$

There are several possibilities for an optimal design. For example, if we minimize the length $L = \ell_1 + \ell_2$, we arrive at the smallest magnet for a given solid angle. On the other hand, one can minimize $L = \ell_1 + \ell_2 + \ell_3 = 2\ell_1 + \ell_2$ and arrive at the smallest overall spectrometer. In Table III, we list the properties of both spectrometers. They are not spectacularly different.

Table III. Forward Spectrometer Parameters.

	I	II
What is minimized	$\ell_1 + \ell_2$	$\ell_1 + \ell_2 + \ell_3$
Magnet length, ℓ_2	16.4 m	23.2 m
Spark chamber separation, $\ell_1 = \ell_3$	16.4 m	11.5
Bend angle, Θ	0.074 rad	0.105 rad
Overall length, $\ell_1 + \ell_2 + \ell_3$	49.2 m	46.2 m
Displacement of central orbit at the magnet exit, $1/2\ \Theta \cdot \ell_2$	0.61 m	1.22 m
Vertical (bend-plane) acceptance, ψ_v	0.02 rad	0.02 rad
Horizontal acceptance, ψ_N	0.01 rad	0.01 rad
Pole-face width	$\simeq$ 0.8 m	$\simeq$ 0.8 m
Magnet gap	$\simeq$ 0.4 m	$\simeq$ 0.4 m
Momentum acceptance, $\Delta p/p$	$\simeq$ 0.25	0.25

Next we must decide on a solid angle. This is difficult to do in a direct manner since it involves counting rates and running time. One choice is to select the angular acceptance in the scattering plane sufficiently large that one accepts the full momentum-transfer range of interest at the lowest incident energy. For $E_{incident} = 20$ GeV and a momentum transfer of 1 GeV, an angular acceptance of 50 mrad is required. With the rear of the magnet approximately 36 m from the target, this would require a magnet aperture of 2 m in one dimension. This appears to be a little too luxurious but not out of the question. As a more modest start, we will consider an acceptance of $\psi_H = 10$ mrad $\times$ $\psi_v = 20$ mrad. We will try to show that this is not an unreasonable choice in view of the rates. The 2 : 1 aspect ratio has been chosen for the convenience of designing magnets with uniform field. I have also introduced another prejudice at this point; namely, I have chosen the bend plane to be vertical. Neither of these assumptions are crucial for what follows but will become important when one considers a supporting structure and how one changes the angular range of interest. The rest of the quantities in Table III are computed on the basis of the 0.01 rad $\times$ 0.02 rad acceptance. (Through the rest of the report, if there is a specific spectrometer parameter required, we will use Case 1.)

Aside from the magnet, the other components of the forward spectrometer are the wire chambers and Cerenkov counters. Wire chambers of the required dimensions are straightforward. Aside from the four shown in Fig. 1, we would install a fifth chamber in the middle of region 2.

In view of the angular divergence of the rays in the spectrometer (±0.014 rad) it is necessary to use threshold Cerenkov counters. Use of multi-alkali photocathodes with their 25-30% quantum efficiency means that one can have an overall quantum efficiency of 20%. If we are willing to settle for 7 photoelectrons then the counter length required to separate 100 GeV/c K's from π's is[1]

$$\begin{cases} N_{photons} = 3 \times 10^4 \, \alpha^2 \, \ell \\ \alpha_\pi^2 - \alpha_K^2 \simeq \dfrac{M_K^2 - M_\pi^2}{p^2} \quad (\text{set } \alpha_K = 0) \end{cases} \tag{9}$$

$$\ell = \frac{N_{photons}}{3 \times 10^4 \left(\dfrac{M_K^2 - M_\pi^2}{p^2} \right)} = \frac{7}{3 \times 10^4 \left(\dfrac{0.25 - 0.23}{104} \right)}$$

ℓ = 10 meters.

If two or more photoelectrons are required for a trigger, so that the counter noise is not bothersome, the probability of missing a pion is 0.75%. A set of four threshold counters in series will be adequate for separating π's, K's, and p's to the degree required. They can be conviently intercalibrated for efficiency and rejection factor. We would expect to put the first Cerenkov counter between the "C" and "D" wire planes shown in Fig. 1. The others go behind "D" making the overall system length ≈ 80 m. The diameter of the last counter would be 2 meters.

IV. ESTIMATE OF THE DATA RATES

Before going into further design details, we want some idea of the rates that will be provided by our choice of spectrometer aperture. To estimate these rates, we must first make an extrapolation of the existing cross sections. We will treat four different processes which will span the range of counting rates.

A. Elastic Cross Sections

For present purposes, the high-energy elastic scattering cross sections at small momentum transfer ($|t| < 1$ GeV/c)^2 can be adequately represented by

$$\frac{d\sigma}{dt} = Ae^{Bt}, \tag{10}$$

where A and B are independent of energy. B lies between 7 and 10 $(GeV/c)^{-2}$ for all processes and A can be related to the total cross sections by the "optical theorem."

Crude estimate of elastic cross sections:

$$A = \frac{1}{16\pi}\,\sigma_{tot}^2 \tag{11}$$

$$\sigma_E \equiv \int_{-\infty}^{0} dt\,\frac{d\sigma}{dt} = \frac{A}{B}. \tag{12}$$

Table IV. Elastic Cross Sections.[2]

Process	σ_{tot} (mb)	A (mb/GeV^2)	B (GeV^{-2})	σ_E (mb)	Comment
p + p	40	80	8	10	Falling slowly
π + p	25	32	9	3.5	Constant
K + p	22	25	8	3.1	Constant
$\bar{p}$ + p	52	135	9	14	Falling slowly

B. Baryon Resonance Production

The experimental situation here is not clear even in the 5 to 20 GeV energy region. There seems to be some experimental evidence to support the following conjunctures:

1. The cross section for production of an I = 1/2 resonance will become constant at high energies since this can take place by Pomeron exhange.

2. At high energies, I = 3/2 production will proceed through ρ exchange. Using $\sigma_\rho(t = 0) = 0.5$, we obtain $\sigma \sim 1/s$.

From the data of Anderson et al.,[3] we take the N^* production cross section in pp collisions as

$$\frac{d\sigma}{dt} = Ae^{Bt};\ \sigma \equiv \frac{A}{B}. \tag{13}$$

Table V. N^* Production in p-p Collisions.

Process	A mb/(GeV/c)^2	B (GeV/c)$^{-2}$	σ (mb)
pp → p + Δ (1.238)	1.7 (10/p_{inc})	17	0.1(10/p_{inc})
pp → p + N (1.40)	6	15	0.4
pp → p + N (1.52)	0.33	3.8	0.088
pp → p + N (1.688)	1.5	5.2	0.29

C. Associated Production

Experimentally, cross sections for a particular channel fall off as $s^{-\lambda}$ with $\lambda \simeq 2.5$ to 3. For example, a fit to the cross section for

$$\pi^+ + p \rightarrow K^+ + \Sigma^+$$

at $p_\pi \simeq 1.6$, 2.6, 4, and 8 GeV[4] gives

$$\sigma_{tot} \simeq 0.06 \left(\frac{p_{lab}}{4} \right)^{-2.8} \text{ mb.}$$

However, the total cross section for $\pi^\pm + p \rightarrow K^+ + Y^\pm$ seems to remain constant at 1.5 mb.[5]

The processes which can take place through strangeness 1 meson exchange are the dominant ones, and they all peak in the forward direction.

D. Baryon Exchange Processes

Data exist on backward[6] distributions for

$$\begin{aligned} \pi^- + p &\rightarrow p + \pi^- \\ &\rightarrow p + \rho^- \\ &\rightarrow p + A_1^- \\ &\rightarrow p + A_2^- \end{aligned} \qquad (14)$$

The differential cross sections decrease as s^{-2} for incident energies of 4 to 16 GeV. We will parametrize the backward elastic cross section [say for $-u < 1$ (GeV/c)^2] as

$$\frac{d\sigma}{du}_E = 3.6 \left(\frac{p}{8} \right)^{-2} e^{+4u} \ \mu\text{b/(GeV/c)}^2 , \qquad (15)$$

$$\sigma_E = \int_{-1\,(\mathrm{GeV}/c)^2}^{u_{min}} du \left(\frac{d\sigma_E}{du}\right) \simeq \frac{50}{p^2\,(\mathrm{GeV})} \ \mu b. \qquad (16)$$

We should keep in mind that the cross sections for the other reactions are comparable.

Backward $\pi^+ p$ has an interesting u dependence which should be studied at high energy. The total backward $\pi^+ p$ cross section $[-u < 1\ (\mathrm{GeV}/c)^2]$ is 5 times larger than $\pi^- p$ at 8 GeV incident momentum and is decreasing as s^{-3}.

The lowest rate experiment we will consider in this note is the 2-pion annihilation of the proton-antiproton system. For pions emitted at forward or backward angles the reaction proceeds mainly by baryon exchange. The angular distribution of the forward π^+ (π^-) is related by s-u crossing to the angular distribution of backward elastic $\pi^- p$ ($\pi^+ p$) scattering.[7] At NAL energies the relation simplifies to

$$\left(\frac{d\sigma}{du}\right)_{\bar{p}p \to \pi^\pm \pi^\mp} = \frac{1}{2} \left(\frac{d\sigma}{du}\right)_{\pi^\mp p \to p\, \pi^\mp} . \qquad (17)$$

In Tables VI(a), b, and c we give approximate counting rates per pulse based on the cross-section estimates. These were calculated from

$$R = n_p N_I \left(\frac{\phi}{2\pi}\right) \sigma\ t_+, t_- , \qquad (18)$$

where

n_p = target thickness, 4×10^{24} protons/cm^2 for 1 meter of hydrogen

N_I = Incident flux taken from Fig. 3 of SS-41 for $\Delta p/p = 10^{-3}$.

$$\tan(1/2\ \phi) = \frac{\psi_v}{2\Theta_{spect}} = \frac{0.01}{\text{mean spectrometer angle}}$$

$$\sigma(t_+, t_-) = \int_{t_-}^{t_+} dt \frac{d\sigma}{dt}$$

t_+, t_- = momentum-transfer squared at the spectrometer edges.

Leaving aside the antiproton reactions, we see that the rates vary by a factor of 10^5 to 10^6. It would be inefficient to attempt to measure all of these simultaneously. Later we will discuss how one would want to proceed. The point we should realize

now is that the rates are adequate. As a rule of thumb we use: 250 events is the minimum number to measure a cross section and 2500 is the minimum for a polarization. (In general we would like to have 50 to 100 times this number.) We assume that we would be taking data for 4 to 6 weeks at a stretch. If we were to run for 1 week at 100 GeV/c at the rates indicated in the table, we would obtain $\approx 10^3$ $\pi^- p \to p\rho^-$ events (I have assumed 10^4 pulse/day). This would provide a good cross-section measurement (10 points on a u distribution, each to 10% accuracy). Actually, we would hope to do better than this by an order of magnitude.

Table VI(a). Approximate Rates at 25 GeV/c, Counts/Pulse.

Incident Beam Intensity:
$N_I = 2.6 \times 10^6$ π's; 4×10^4 K^+; 4×10^4 $\bar{p}$/pulse

Spectrometer Angular Range:	0-10 (mrad)	10-20 (mrad)	20-30 (mrad)	30-40 (mrad)
Momentum Transfer	0-0.25 (GeV/c)	0.25-0.5 (GeV/c)	0.5-0.75 (GeV/c)	0.75-1.0 (GeV/c)
$\pi p \to \pi p$	12×10^3	650	45	3.9
$K^+ p \to K^+ p$	151	10.8	1.0	0.1
$\pi p \to \pi N^*(1238)$	250	18	1.6	0.16
$\pi p \to \pi N^*(1688)$	780	56	5	0.5
$\pi^- p \to K^+ \Sigma^-$	1.2	0.08	0.0074	0.00074
$\pi^- p \to p\rho^-$	0.2	0.04	0.0095	0.0026
$\bar{p}p \to \pi^+ \pi^-$	0.9×10^{-3}	0.18×10^{-3}	0.04×10^{-3}	0.01×10^{-3}

Table VI(b). Approximate Rates at 50 GeV/c, Counts/Pulse.

Incident Beam Intensity:

$N_I = 3.4 \times 10^6$ π; 1.4×10^5 K^+; 3.2×10^4 $\bar{p}$/pulse

Spectrometer Angular Range:	0-10 (mrad)	10-20 (mrad)
Momentum Transfer	0-0.5 (GeV/c)	0.5-1.0 (GeV/c)
$\pi p \to \pi p$	17×10^3	91
$K^+ p \to K^+ p$	600	6
$\pi p \to \pi N^*(1238)$	187	1.9
$\pi p \to \pi N^*(1688)$	1170	12
$\pi^- p \to K^+ \Sigma^-$	0.25	0.0026
$\pi^- p \to p \rho^-$	0.18	0.013
$\bar{p}p \to \pi^+ \pi^-$	0.5×10^{-3}	0.035×10^{-3}

Table VI(c). Approximate Rates at 100 GeV/c, Counts/Pulse.

Incident Beam Intensity:

$N_I = 1.7 \times 10^6$ π; 1.6×10^5 K^+; 1.6×10^4 $\bar{p}$/pulse

Spectrometer Angular Range:	0-10 (mrad)
Momentum Transfer	(0-1.0 GeV/c)
$\pi p \to \pi p$	8.5×10^3
$K^+ p \to K^+ p$	700
$\pi p \to \pi N^*(1238)$	48
$\pi p \to \pi N^*(1688)$	600
$\pi^- p \to K^+ \Sigma^-$	0.015
$\pi^- p \to p \rho^-$	0.013
$\bar{p}p \to \pi^+ \pi^-$	0.035×10^{-3}

V. THE VERTEX DETECTOR

The vertex detector is supposed to provide

1. Additional identification of the reaction.
2. Branching ratios for the decay of particle D.
3. Improved mass resolution on particle D.
4. Information on the polarization of particle D through the angular distribution of the decay.

It is not clear how to arrive at an optimal configuration from first principles. In fact, it is even difficult to show that a particular design is adequate. We will try to motivate the configuration we have chosen and then show what this buys.

1. Most of the events that we will be studying will have particle D emitted at a polar angle between 45° and 150°. For example, if A and C are pions and if $|t| \leq 1$ and $M_D < 1.5$ GeV, the polar angle lies between 50° and 90°.

2. The momentum of particle D is less than 1 GeV/c if it is emitted into the backward hemisphere. If particle D is emitted in the forward hemisphere, its momentum may be larger than 1 GeV/c, but its transverse component will be less than 1 GeV/c for $|t| < 1$.

3. The maximum momentum of the decay products of particle D is less than 1.5 GeV/c if $p_D \leq 1$ GeV/c and $M_D \leq 1.5$ GeV.

Therefore, we should be prepared to measure transverse components of momenta up to $\simeq 1$ GeV/c to some required accuracy.

4. In doing an energy-momentum balance to look for missing neutrals, the transverse component of momentum is the most sensitive test one can generally make.

5. For polarization information on particle D, one needs to detect its decay in $\simeq 4\pi$ geometry.

6. In looking through the list of reactions in Table I, it would not be necessary to detect the π^0 decay photons, since all listed cases for particle D have reasonable (say > 10%) branching ratios into either charged + neutral or 3 charged particles. (One would have to know the branching ratio into this channel.) On the other hand, it would be very desirable to at least pick up the photon directions.

Since we want to measure the transverse component of the momentum, we will arbitrarily impose the criteria that the resolution in this measurement be compatible with the measurement made in the forward spectrometer. In the latter, we measure the momentum to an accuracy $\delta p/p \simeq 10^{-3}$ and the scattering angle to an accuracy of 2×10^{-4} rad. (This is set by the divergence of the incident beam.) Then

$$p_{TR} = p\Theta$$

$$\delta p_{TR} = (p\Theta)\frac{\delta p}{p} + p\delta\Theta .$$

Using $p\Theta$ = 1 GeV/c and p = 100 GeV/c to obtain some typical numbers, we have

$$\delta p_{TR} = \left[\left(10^{-3}\right)^2 + \left(2 \times 10^{-2}\right)^2\right]^{1/2} ,$$

and we see that the uncertainty in the scattering angle generally limits the accuracy of the transverse momentum measurement to δp_{TR} = 20 MeV/c. If we want to measure a 1 GeV/c transverse momentum to this accuracy in the vertex detector using a sagitta method in a field B = 15 kG with a spatial resolution of $\delta s = \pm 0.3$ mm = 0.6 mm, we require a track length, ℓ, of

$$\ell^2 = \frac{8\,p_{TR}(\delta s)}{(eB)\left(\frac{\delta p_{TR}}{p_{TR}}\right)}$$

$$\ell^2 = \frac{8\left(10^9\right)\left(0.6 \times 10^{-3}\right)}{\left(1.5 \times 3 \times 10^8\right)\left(2 \times 10^{-2}\right)}$$

$$\ell^2 = 0.53$$

$$\ell^2 = 0.73 \text{ m}.$$

With this as a guide, we propose to make the magnetic field of the vertex detector extend 1 meter in every direction about the target center. Later, we will check how well we satisfy the other criteria for the detector. Since we are primarily interested in the transverse momentum, and since the preferred direction for the low-momentum particles in the processes we are studying is perpendicular to the beam line, it would be sensible to have the magnetic-field lines lie along the beam direction. Therefore, we propose to make a magnetic field 2 m in diameter and 2 m in length, with the field lines parallel to the beam. In Fig. 2 is shown a schematic of the geometry. The beam is brought in through a 10 cm hole in the front pole tip. Forward reaction products exit through a conical aperture in the rear pole tip (30 cm on the inside and 40 cm on the outside) with an angular opening greater than ±0.1 radians for a point inside the target. The coils fill the magnetic gap in a geometry which assures field homogeneity. A 10-inch space has been left clear in the middle of the coils to

allow access for hydrogen-target lines and electrical cabling. These could be brought in through holes in the iron return yoke.

The magnetic field region would be filled up with wire chambers (probably of the Charpak variety). If the fabrication of cylindrical wire chambers is practical, one would use them with a plane chamber on each end. Figure 3 shows such a configuration. It should be noted that the outermost wire chambers could be constructed as shower chambers so that one obtains the direction of the π^0 photons without loss of momentum resolution. The wire chambers could be supported either from the pole tips or from the return yokes. Installation and servicing would be done by removing the pole tips.

The transverse-momentum resolution is 2% at 1 GeV/c. This improves linearly with decreasing p_{TR} until the particle is trapped in the magnetic field (this occurs at $p_{TR} \simeq 225$ MeV/c at which point the resolution is $\delta p_{TR}/p_{TR} \simeq 0.3 \times 10^{-2}$). For lower momentum, the resolution decreases as $\simeq 1/p_{TR}$ until a multiple-scatter limit sets in. Particles of $\tilde{<} 10$ MeV/c are magnetically trapped in the target.

The angular resolution is somewhat momentum-dependent. Leaving aside multiple scattering in the target, the resolution on the polar angle (relative to beam line) is

$$\delta\Theta \simeq \frac{\sqrt{2}\,\delta x}{\ell} \cdot \frac{\sqrt{2}\ 0.6 \times 10^{-3}}{0.7} = 1.2 \times 10^{-3} \text{ rad.}$$

(Perhaps a realistic number would be twice this, i.e., $\delta\Theta = \pm 1.2 \times 10^{-3}$ rad.)

To know the azimuthal angle, one must locate the vertex. This depends on an extrapolation of another charged particle, for example, the high-momentum forward particle C. We can assume we lose another factor of 2 in the extrapolation and use

$$\delta\phi = \pm 2.4 \times 10^{-3} \text{ radian.}$$

With a definite piece of apparatus in mind, we can see how well it performs its various functions. First consider elastic $\pi^- p$ scattering for $p_{inc} = 100$ GeV/c and $t = 1\,(\text{GeV/c})^2$. The problem is to discriminate against the final states $\pi^-(N\pi^+)$ and $\pi^-(p\pi^0)$. From the measurement of the momentum and angle of the π^- in the forward spectrometer, we know the low-momentum particle (particle D) has the following properties:

$$p_D = 1.13 \pm 0.04 \text{ GeV/c}$$
$$M_D^2 = M_p^2 \pm 0.15$$
$$(0.85 < M_D < 1.01 \text{ GeV})$$
$$\Theta_D = 61.7^\circ .$$

From this we can already rule out particle D being a nucleon plus pion. However, for large t values [like t = 1 $(GeV/c)^2$], it will be important to have good discrimination for events out in the tail of the distribution. Therefore, we will consider an event which is 3 standard deviations out in the tail and look at the momentum and angle relationship of the proton relative to particle D for a ($p\pi^o$) system of mass M_D = 1.16 GeV. This is shown in Fig. 4. Also shown in this figure is the point for the proton from elastic scattering. The shaded area represents the uncertainty of 1 standard deviation. To estimate the factor by which we reduce the background, we first take into account the azimuthal angle measurement (coplanarity). The forward π^- angle is $\Theta_{\pi^-} = 0.01$ rad so that one measures its azimuth angle to $\delta\phi_\pi = \pm 1.5\times10^{-3}$. Using $\delta\phi_p = \pm 2.4 \times 10^{-3}$ for the proton, we get for the combined uncertainty $\delta\phi = 2.64 \times 10^{-3}$. Using three standard deviations, the rejection factor is $\simeq$ 30 (note, I have assumed the proton came off at $\simeq 7°$ relative to particle D). Next we estimate the rejection factor from the momentum angle measurement will be about $\simeq$ 15. So the background under the π^- elastic peak from ($p\pi^o$) at a point 3 standard deviation away is reduced to 0.2%. The background from the (π^+N) state is even smaller since the π^+ momentum is always less than 0.5 GeV/c.

In Fig. 5 is shown the same type results for backward π - p scattering. In this case one detects the proton in the forward spectrometer and determines u = 1 $(GeV/c)^2$ and $M_D^2 = M_\pi^2 \pm 0.15$ GeV^2 ($0 < M_D < 0.39$ GeV). This does not rule out the 2-pion state for particle D. However, measurement of the π^- direction and momentum in the vertex detector gives $\simeq$ 6 standard deviation discrimination against the 2-pion state.

As a final example of the value of the vertex detector, we consider a reaction which makes use of the 4π acceptance. This will also illustrate some of the limitations of the device. Assume that we wish to measure the cross section and polarization dependence of backward $\pi^-p \to p\rho^-$. We will estimate the discrimination against the final state $p\pi^-\pi^o\pi^o$. Again we take an incident energy of 100 GeV/c, but we consider u = -0.25 $(GeV/c)^2$ as more typical of a region in which one has not run out of rate. From the momentum-angle measurement in the forward spectrometer we determine

$$p_D = 0.50 \pm 0.02$$
$$M_D^2 = 0.58 \pm 0.15$$
$$\Theta_D = 92° \pm 9.$$

In Fig. 6 we show the locus of the π^- from the ρ^- decay in the p vs ψ plane. In addition is shown the boundary of the π^- from a final state of $\pi^-\pi^o\pi^o$. As shown in the

figure, these regions are distinct. However, when one includes the measuring errors in the forward spectrometer, the boundaries broaden and overlap. Taking into account that the π^- from the 3π state is preferentially found near the boundary, one estimates the rejection factor provided by the vertex detector is only $\simeq 10$. If one needed better discrimination, the direction of the π^o decay photons would provide this.

VI. VARIATION OF THE ANGULAR RANGE COVERED BY THE FORWARD SPECTROMETER

Since the angular acceptance of the forward spectrometer does not cover the entire range of interesting momentum transfer, it will be necessary to vary the angular range. This can be done in one of several ways.

1. A rigging crew can disassemble the spectrometer and rebuild it at a new angle.

2. The spectrometer can be mounted on wheels set up on tracks and motor driven over some reasonable angular range (10° to 15°).

3. The incident beam can be steered with a two-magnet system to vary the beam direction relative to the spectrometer.

System (1) is useful in the case where one contemplates a single move during the course of the experiment. Since we look upon the spectrometer as a semi-permanent facility to be used for many experiments, we dismiss the idea of using riggers.

System (3) is especially suited to the program discussed here namely, momentum transfers of 1 GeV/c or less. To obtain this type of bend requires

$$B\ell = \frac{p\theta}{e} = 33 \text{ kG-meter},$$

which could be provided by a 2-meter long magnet. Furthermore, the aperture requirements for this magnet plus a smaller one upstream are only a few inches. The usual disadvantage of bending the incident beam is one of understanding and maintaining the beam phase space and halo after the bend. However, with a well-designed beam line, this should not be too much of a problem.

For the experimental setup we are proposing in this report, system (2), rotating the spectrometer, offers several advantages.

1. One can build in a lot of extra angular range at no extra cost (once you have paid the initial price).

2. The angle of the beam relative to the vertex detector is fixed. This makes analysis programs simpler and faster. [One could have this when rotating the beam, method (3), if one simultaneously rotated the vertex detector. However, it seems simpler to rotate the spectrometer.]

Also we should make the argument that mechanical rotation is more reproducible (and therefore more reliable). Furthermore, the problem of beam dumping and personnel safety are minimized.

The question immediately comes up as to the feasibility or rotating a magnet-counter system of 80 meters length with the precision called for in this proposal. As a good example of such a rotating support system, one need only turn to the SLAC 20-GeV spectrometer which is 50 meters in length. The alignment tolerances on the SLAC spectrometer are slightly tighter than those we require since the system contains quadrupoles. In general, an alignment of ±0.003 to 0.005 inches is maintained over the entire length. A roll angle of less than $\pm 2 \times 10^{-5}$ radians is maintained on the individual elements.

There does not appear to be any strong reason to choose between (2) and (3). We prefer (2) for the advantages stated although the initial cost is higher. (The cost of rotating the SLAC spectrometer was $120K. The 20-GeV magnet weight is ~360 tons compared to an estimated weight of 170 tons for this beast.)

VII. DATA RECORDING RATES AND ON-LINE ANALYSIS

The wire chambers that we have described could be conventional magnetostrictive or core readout. However, the Charpak chambers offer the opportunity of operating at higher data rates. Therefore, we will assume that we can use these and see what it will entail. The system will have about 50,000 wires. These will have to be read into a computer memory. The SDS 9300 (not necessarily the ideal device but one with which the author is familiar) uses a 24-bit word and has a 0.75 μsec cycle time. It will require 1.5 to 2 msec to read in all the data. If one were to operate at 30% computer dead time, the trigger rate must be limited to 150/sec. There are ways to speed things up such as fast computers or parallel input systems. However, 150/sec is a reasonable rate provided a non-vanishing fraction are interesting events. We will discuss the triggering system later.

Personal experience has shown that there are many advantages to having on-line analysis which is sufficiently complete to give the experimenter cross sections on all or most of the processes he is monitoring. This is possible by using an "interrupt-oriented computer" and sampling. When an event occurs, it is immediately read into the computer buffer. The buffer should be large enough to handle ~20 events. (The information stored in the buffer would be the coordinates of every pulsed wire. The coordinates of one wire require only 16 bits. Assuming 6 or less charged tracks, this would mean that we would need to reserve ≃ 60 words per event.) After 20 events have been read, the computer switches to a second buffer and the contents of the first buffer are read onto magnetic tape. Meanwhile, between events the computer begins

analyzing the last event. If another event comes in before the analysis is completed, the new event is read into the buffer and then the computer returns to the analysis. Since the accelerator cycle is 1 second "on" followed by 3 seconds "off," one could arrange to have the computer analyze the contents of the last buffer during the off time.

This type of system will work provided the analysis of a single event can be done in 50 msec. In all of the reactions in Table I (except possibly some Y^* production), the low-momentum system (particle D) has a significant (> 30%) branching ratio into one charged plus one neutral. For these decay channels, there would appear one charged track for the high-momentum particle and one for the low-momentum particle. These events could easily be recognized and analyzed on line. We have estimated about 20 msec of SDS 9300 computer time would be required to analyze such an event. In this way, one could sample more than 30% of the events and have immediate cross-section information on all reactions of interest.

VIII. BEAM RATE LIMITATIONS

We have already seen that one is limited to ~150 triggers per second by the ability of the computer to read the data into a buffer. If one triggered on all forward-going particles, the elastic pion events would swamp the data-reading capability. We will shortly discuss selective triggering. In this section we want to see what are the other limitations on beam rates.

In Reeder's beam design (SS-41), he expects ~ 2×10^6 π's/pulse in a 0.1% momentum bin. One can open the momentum slits to 2% and obtain an additional factor of 20. It is not necessary to lose the precise momentum information, since one could tag the particles at the momentum crossover (momentum dispersion plane) in the beam transport.

The limitation of the system is likely to be in the vertex detector. With 2×10^7 π's/sec passing through 1 meter of hydrogen there will be 2×10^6 interactions/sec. If the wire chambers have a 1-μsec memory there will be 2 additional events in the vertex detector on each trigger. Therefore, the normal wire chamber (with restrictive line or core readout) limits the incident beam rates to ~2×10^6/sec.

The Charpak chamber offers another decade in allowed beam intensities. These chambers can be run with 50-100 nsec resolving time[8,9] and repetition rates of 2×10^5 per wire. With 2×10^6 interactions per second, one would have an extra event in the vertex chambers in only 10% or 20% of the triggers.

IX. DATA-TAKING PHILOSOPHY

The range of rates given in Table VI is far too great to profitably take data on all reactions simultaneously. The rates for the first 4 reactions (especially elastic

pion scattering) are so great that one would use up all the data-recording capability on these without obtaining a significant amount of data on the last three reactions. It would be better to initially concentrate on the high-rate reactions. For these one would drop the beam intensity a factor of 10 to 100 from the values in the table. After one completed a series of experiments on the low-t, non-strangeness-changing reactions, one could raise the beam intensity a factor of 5 to 10 above the values in Table VI and measure the other reactions (low u, i.e., baryon exchange and strange meson exchange).

The ability to measure the low cross-section reactions at high beam intensities depends on one's ability to selectively trigger on the reactions of interest. The baryon-exchange reactions listed in Table I are all characterized by a forward proton. (The one exception is $\bar{p}p \to \pi\pi$ or KK in which an antiproton turns into a fast forward meson.) The strange-meson exchange reactions of Table I are characterized either by an incoming pion changing into a forward kaon or vice versa. By using fast hardware logic on the Cerenkov counters in the incident beam line and in the forward spectrometer, one can take advantage of these characteristics to selectively trigger on low cross-section events.

We conclude, therefore, that although the apparatus, in principle, measures all reactions simultaneously, one should expect to make two or three passes using various Cerenkov triggering requirements to isolate those reactions which can be measured at comparable beam intensities.

X. COSTS

On the basis of the ideas described here, we have tried to estimate the cost of the hardware needed for this program. (No attempt has been made to cost the subcomponent parts in detail, and the numbers shown can only be used as a rough guideline.) In Table VII we give the numbers for various components and the basis on which they were costed.

Considering what is shown in Table VII (a total of M $3.6), we would estimate that the total costs over 3 years of construction plus 5 years of operation will be M $5 to M $6.

Table VII. Cost of Hardware

	Components	Basis for Cost Estimate	Cost, M$
1.	Forward spect. magnet	$5,000 capitalization per cu. ft of field (magnet + power supply) (See D. H. White, 1968 Summer Study)	0.9
2.	Support and rotate spect.	Based on cost of same for SLAC 20-GeV spectrometer	0.1
3.	Vertex magnet	Same as (1)	1.1
4.	Threshold Cerenkov ctrs.	$25,000/counter, 4 counters (does not include differential counters needed in the beam transport)	0.1
5.	Wire planes	50,000 wires at $8/wire includes discriminator-univibrator and gate on each wire	0.4
6.	Electronics	Buffers for wire plane read out (M$0.1); fast trigger logic (M$0.05); pulse height analysis, gating, etc. (M$0.05)	0.2
7.	Computer	Cost of SDS-9300 (including 3 mag. tapes, 2 disc packs, card reader, line printer, teletype, and scope) is ≈ M$0.5	0.8
		TOTAL	M$3.6

FOOTNOTE AND REFERENCES

†Present address: Laboratory of Nuclear Studies, Cornell University, Ithaca, New York.

[1] CERN/ECFA-67, Vol. 1, Jan., 1967, p. 357.

[2] K. Foley et al., Phys. Rev. Letters 15, 45 (1965) (see this paper for earlier work).

[3] E. W. Anderson et al., Phys. Rev. Letters 16, 855 (1966).

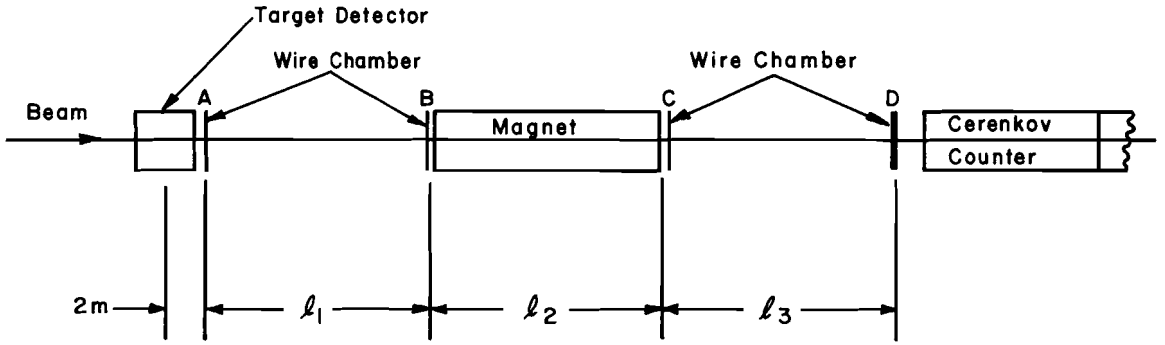

Fig. 1. Forward spectrometer layout.

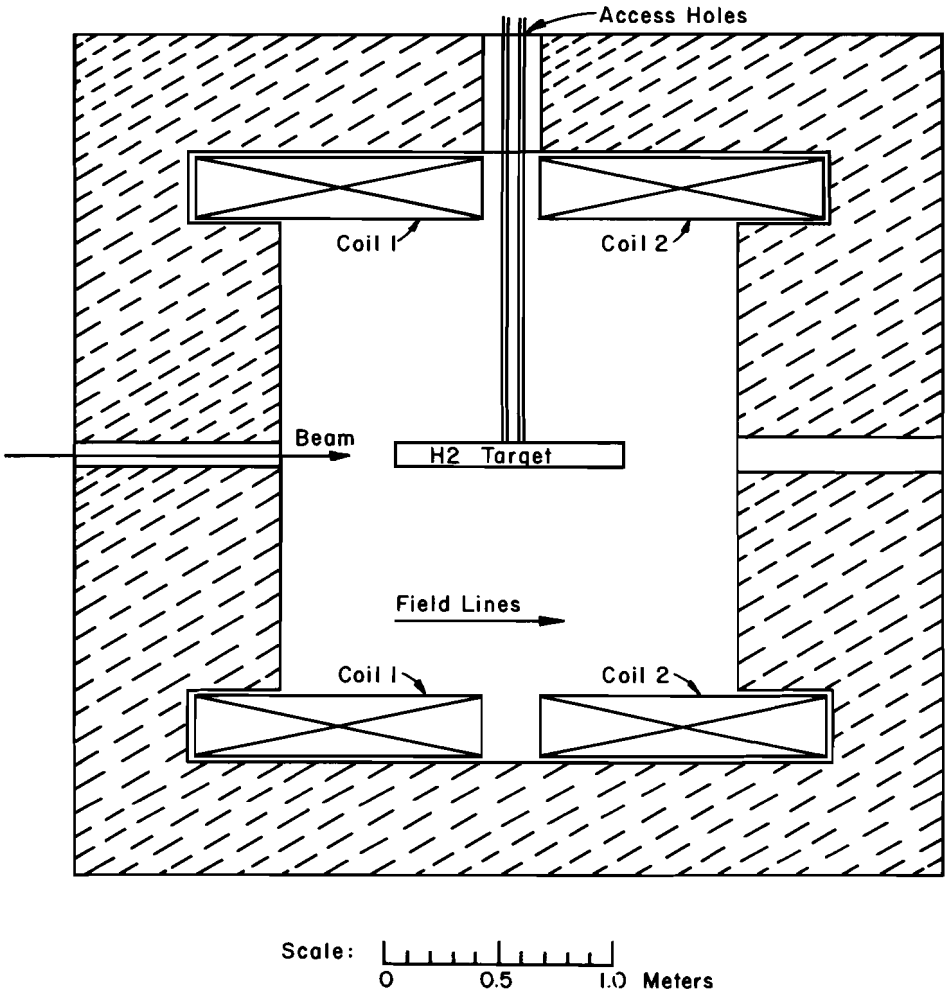

Fig. 2. Vertex detector magnet.

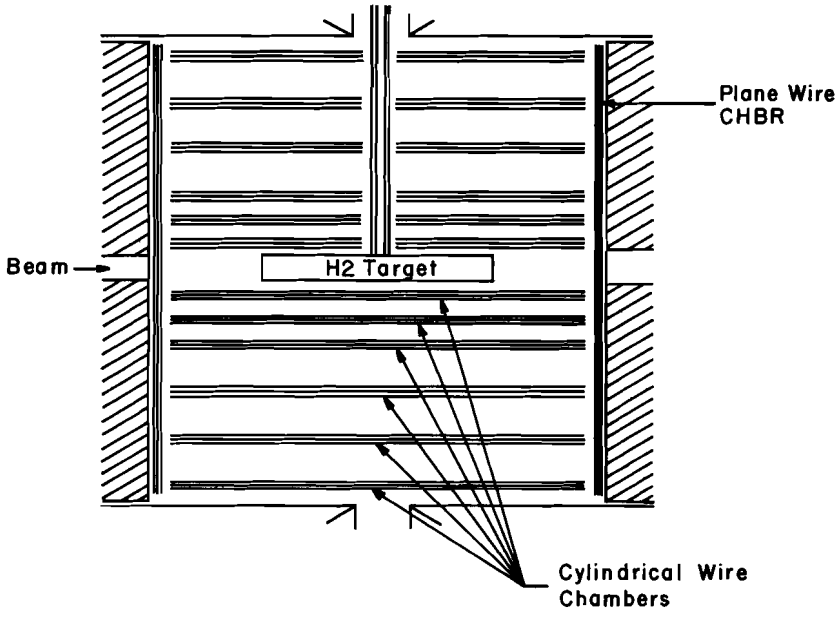

Fig. 3. Vertex detector spark-chamber array.

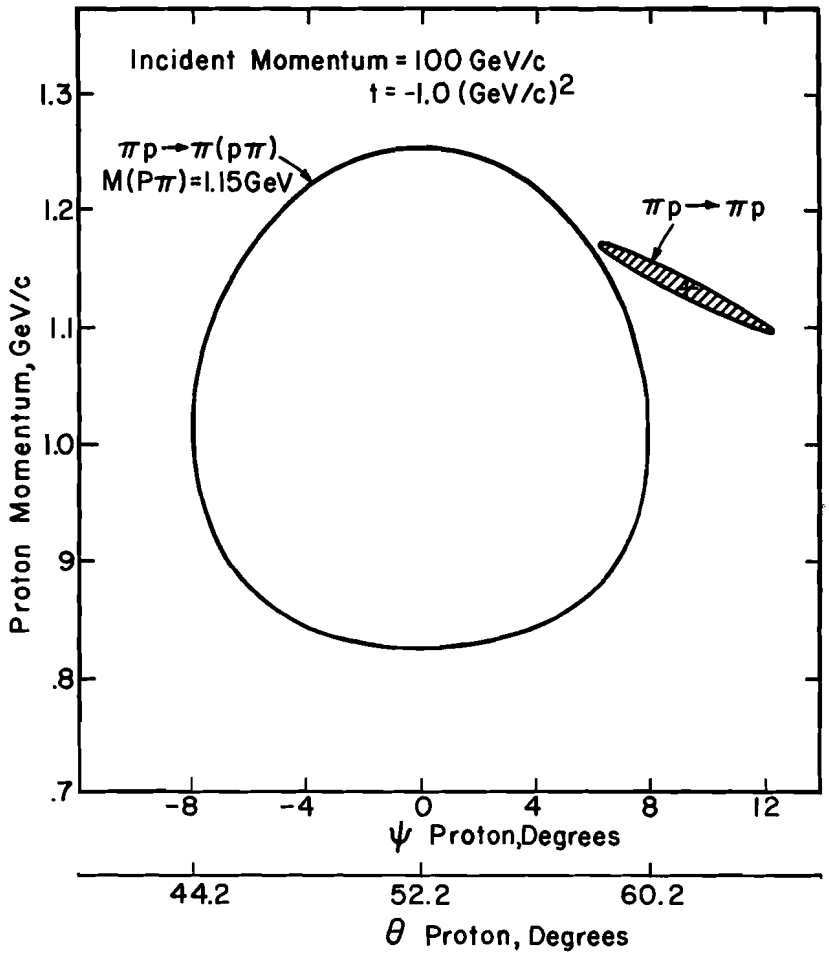

Fig. 4. Proton kinematics for $\pi^- + p \rightarrow \pi^- + (p\pi^o)$.

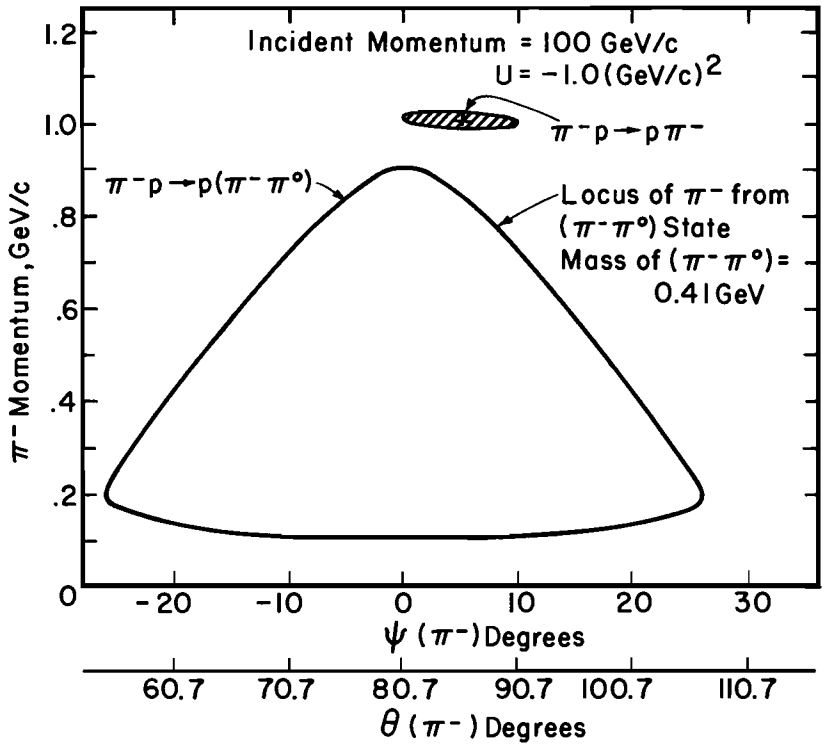

Fig. 5. π^- kinematics for $\pi^-p \to p + (\pi^-\pi^o)$.

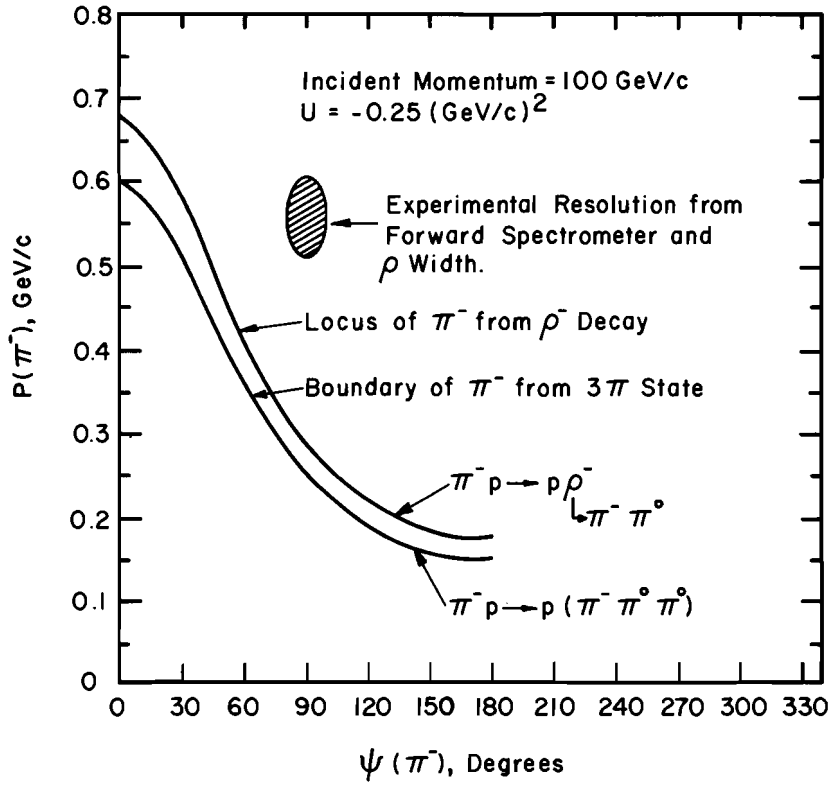

Fig. 6. π^- kinematics for backward ρ^- production.